INFECTION AND IMMUNITY, Aug. 2003, p. 4351–4360 Vol. 71, No. 8
0019-9567/03/$08.00+0 DOI: 10.1128/IAI.71.8.4351–4360.2003

Effect of an Orphan Response Regulator on *Streptococcus mutans* Sucrose-Dependent Adherence and Cariogenesis

Vincent Idone,[1] Stacy Brendtro,[1] Robert Gillespie,[1] Steve Kocaj,[1] Erica Peterson,[1] Mara Rendi,[1] Wayne Warren,[1] Suzanne Michalek,[2] Kirsten Krastel,[3] Dennis Cvitkovitch,[3] and Grace Spatafora[1]*

Department of Biology, Middlebury College, Middlebury Vermont 05753[1]; Department of Microbiology, University of Alabama at Birmingham, Alabama 35294[2]; and Dental Research Institute, University of Toronto, Toronto, Ontario, Canada M5G 1G6[3]

Received 12 March 2003/Returned for modification 27 March 2003/Accepted 15 April 2003

Streptococcus mutans **is the principal acidogenic component of dental plaque that demineralizes tooth enamel, leading to dental decay. Cell-associated glucosyltransferases catalyze the sucrose-dependent synthesis of sticky glucan polymers that, together with glucan binding proteins, promote *S. mutans* adherence to teeth and cell aggregation. We generated an *S. mutans* Tn*916* transposon mutant, GMS315, which is defective in sucrose-dependent adherence and significantly less cariogenic than the UA130 wild-type progenitor in germfree rats. The results of sodium dodecyl sulfate-polyacrylamide gel electrophoresis, Western blotting, and N-terminal sequence analysis confirmed the absence of a 155-kDa glucosyltransferase S (Gtf-S) from GMS315 protein profiles. Mapping of the unique transposon insertion in GMS315 revealed disruption of a putative regulatory region located upstream of *gcrR*, a gene previously described by Sato et al. that shares significant amino acid identity with other bacterial response regulators (Y. Sato, Y. Yamamoto, and H. Kizaki, FEMS Microbiol. Lett. 186: 187-191, 2000). The *gcrR* regulator, which we call "*tarC*," does not align with any of the 13 proposed two-component signal transduction systems derived from in silico analysis of the *S. mutans* genome, but rather represents one of several orphan response regulators in the genome. The results of Northern hybridization and/or real-time reverse transcription-PCR experiments reveal increased expression of both Gtf-S and glucan binding protein C (GbpC) in a *tarC* knockout mutant (GMS900), thereby supporting the notion that TarC acts as a negative transcriptional regulator. In addition, we noted that GMS900 has altered biofilm architecture relative to the wild type and is hypocariogenic in germfree rats. Taken collectively, these findings support a role for signal transduction in *S. mutans* sucrose-dependent adherence and aggregation and implicate TarC as a potential target for controlling *S. mutans*-induced cariogenesis.**

Dental caries continues to pose an important health problem worldwide. Populations at high risk in the United States include increasing numbers of older Americans who retain their teeth but experience reduced salivary flow owing to long-term medication (43a). *Streptococcus mutans* is the principal causative agent of dental caries in humans, and its ability to adhere to the tooth surface is paramount for the progression of disease (26). Specifically, the sucrose-dependent adherence of *S. mutans* to teeth ensures that bacteria will not be washed away with chewing or the flow of saliva. Bacterial proteins that mediate this interaction with the host are therefore often targeted as vaccine candidates.

The development of dental plaque is pioneered by *Streptococcus sanguis, Streptococcus oralis*, *Streptococcus gordonii,* and *Streptococcus mitis*, followed by colonization by the lactobacilli and other members of the mutans streptococci (19, 33). Structural data obtained by confocal microscopy indicate that plaque, like other mixed biofilm communities, develops as microcolonies separated by water channels that allow soluble nutrients to access cells deep within the biofilm and metabolic waste products to be released (5). In fact, *S. mutans* comprises the primary acidogenic component of dental plaque, where it metabolizes exogenous dietary carbohydrates, including sucrose, and generates lactic acid as a by-product (9, 26). Ultimately, the accumulation of lactic acid in the plaque biofilm results in a localized drop in pH and subsequent demineralization of tooth enamel, marking the onset of dental decay.

When *S. mutans* makes contact with salivary glycoproteins that coat the tooth surface, two stages of adherence follow to mediate development of the plaque biofilm. The first stage is reversible and sucrose independent, involving ionic and lectin-like interactions between bacterial surface antigens, such as protein P1, and host-derived factors in the coat pellicle (15, 22). When dietary sucrose becomes available in the oral cavity, however, cell-associated glucosyltransferases mediate the tenacious adherence of *S. mutans* to the tooth surface by synthesizing water-soluble and -insoluble glucans (21). Namely, the *S. mutans gtfB* and *gtfC* genes encode enzymes that synthesize water-insoluble glucans with predominantly α1,3 linkages, whereas the *gtfD* gene codes for a glucosyltransferase S enzyme (Gtf-S) that produces water-soluble glucans with α1,6 linkages (10, 26). Glucans can also interact with surface-associated glucan binding proteins (Gbps) to promote cell-to-cell aggregation (8), thereby contributing to the cohesive properties of dental plaque. Importantly, the insertional inactivation of genes that encode *S. mutans* glucosyltransferases and glucan binding proteins can alter plaque structure and cariogenesis (11, 30, 47); however, the factors that regulate expression of

* Corresponding author. Mailing address: Department of Biology, Middlebury College, Middlebury, VT 05753. Phone: (802) 443-5431. Fax: (802) 443-2072. E-mail: spatafor@middlebury.edu.

TABLE 1. Bacterial strains and plasmids used in this study

Strain or plasmid	Genotype or phenotype[a]	Source or reference
Strains		
Streptococcus mutans		
UA130	*S. mutans* wild-type (serotype c), adherence proficient, cariogenic	P. Caufield
GMS315	UA130::Tn*916* Tc^r, adherence deficient, hypocariogenic	This work
GMS900	UA130::ΩKm *tarC* Km^r, forms aggregates, hypocariogenic	This work
Escherichia coli DH5α	F^- *adnA1 hsdR17* (r_K^- m_K^+) *supE44 thi-1 recA1 gyrA96 relA1D* (*lacZY-argF*) *U16980d*(*lacZ*) DM15	Sambrook
Plasmids		
pAM620	pVA891::pAD1*Eco*RIF′::Tn*916* Em^r Tc^r	D. Clewell
pCR2.1	3.9-kb TA cloning vector, Km^r Ap^r	Invitrogen
pGEM-T-Easy	3.0-kb TA cloning vector, Ap^r	Promega
pUC19	2.7Kb cloning vector, Ap^r	Promega
pMB12	pGEMT-Easy-derived, harbors the *tarC* gene cloned on an 1.3-kb amplicon, Ap^r	This work
pUC4ΩKm	2.7-kb pUC-derived vector, harbors a 2.1-kb ΩKm-2 cassette, Km^r Ap^r	M. Caparon
pKO	pMB12-derived, contains 2.1-kb ΩKm cassette cloned into the unique *Mfe*I restriction site within the *tarC* coding sequence, Km^r Ap^r	This work
pRG.2	pKO digested with *Pvu*I so as to disrupt the β-lactamase gene, Km^r Ap^s	This work

[a] Em, erythromycin; Tc tetracycline; Ap, ampicillin; Km, kanamycin.

these mediators of *S. mutans* sucrose-dependent adherence and biofilm formation remain to be determined.

The present study investigates a putative response regulator that influences *S. mutans* adherence and subsequent biofilm formation by modulating the production of water-soluble glucans and glucan binding proteins. Specifically, we isolated an adherence-deficient mutant of *S. mutans*, GMS315, that harbors a unique transposon insertion at a locus we call "*tar*," for "tenacious adherence regulator." We noted that GMS315 is significantly hypocariogenic relative to the wild-type in a germfree rat model, and that it is missing a 155-kDa protein, which we identified as Gtf-S by Western blotting and N-terminal sequencing. We identified an open reading frame (ORF) at this locus that shares significant amino acid identity with other bacterial response regulators and that Sato et al. previously characterized as *gcrR*, a regulator of *S. mutans gbpC* expression (39). Herein, we present evidence that supports the *gcrR* gene product, which we call "*TarC*," as a putative transcriptional regulator of *S. mutans gtfD* and glucan binding protein C (*gbpC*), as well as a potential target for controlling the appropriate formation of the plaque biofilm and subsequent cariogenesis.

MATERIALS AND METHODS

Strains. The bacterial strains and plasmids used in the present study are described in Table 1.

Culture conditions. *Escherichia coli* was grown overnight at 37°C in L broth (Difco) with gentle aeration and stored in L broth supplemented with 20% glycerol at −20°C or −80°C. Kanamycin or ampicillin selection was included in the medium when appropriate at a final concentration of 100 μg/ml.

S. mutans was grown as standing overnight cultures at 37°C and 5% CO_2 in Todd Hewitt broth (THB) (Difco) and stored in THB supplemented with 20% sterile glycerol at −20°C or −80°C. The THB used to grow *S. mutans* GMS315 was supplemented with tetracycline at a final concentration of 10 μg/ml. *S. mutans* GMS900 was grown in THB supplemented with 500 μg of kanamycin per ml. *S. mutans* cells were grown in THB supplemented with 1% sucrose for characterization of growth, adherence assays, and scanning electron microscopy (SEM). For isolation of whole-cell protein and total intact RNA, *S. mutans* cultures were grown in the absence of sucrose in THB supplemented with 0.3% yeast extract (THYE).

DNA isolation. *S. mutans* chromosomal DNA was isolated by a modification of the method of Marmur (28) and purified by cesium chloride-ethidium bromide gradient ultracentrifugation. Plasmid DNA was isolated from *E. coli* by Miniprep spin column chromatography according to the recommendations of the supplier (Qiagen).

Restriction digests. Plasmid DNA was digested in 20-μl volumes at 37°C for 2 h or in accordance with the recommendations of the manufacturer (Promega). Chromosomal DNA digests were performed overnight at 37°C in 30-μl volumes.

Transposon mutagenesis. The *E. coli* plasmid pAM620 (Table 1), which harbors the streptococcal transposon Tn*916*, served as an efficient delivery vehicle for the generation of a *S. mutans* transposon library (40). Ten micrograms of pAM620 was used to transform *S. mutans* UA130 as previously described (43). Over 3,000 transposon mutants selected on TH agar plates supplemented with 10 μg of tetracycline per ml were screened for adherence to borosilicate glass tubes as described below.

Adherence and biofilm assays. Adherence to borosilicate glass was assessed according to the method of Murchison et al. (31). Briefly, *S. mutans* wild-type and mutant strains were monitored for adherence to the walls of borosilicate glass tubes following overnight growth in THB supplemented with 1% sucrose. After vigorous vortexing for 10 s, nonadherent planktonic cells were decanted with the supernatant. The remaining adherent cells were visualized on the walls of the tube after staining with crystal violet for 1 min and rinsing with distilled water.

Putative *S. mutans* mutants were evaluated for sucrose-dependent adherence to saliva-coated hydroxyapatite after a 3-h incubation period at 37°C with gentle rotation as previously described (22). UA130 and GMS315 culture supernatants containing nonadherent cells were serially diluted in 0.04 M KCl buffer containing 1 mM phosphate, 0.1 mM $MgCl_2$, and 1 mM $CaCl_2$ and plated onto TH agar plates with appropriate antibiotic selection. Following overnight incubation at 37°C and 5% CO_2, the number of CFU recovered per milliliter of supernatant was obtained and analyzed by using a nonparametric sign test.

Quantification of plaque biomass was performed by the crystal violet release assay as previously described (2).

SEM. SEM was used to examine mid-logarithmic-phase cells of *S. mutans* UA130 and GMS315 and to visualize the architecture of *S. mutans* UA130 and GMS900 biofilms formed on the surfaces of Thermanox coverslips (Electron Microscopy Sciences, Ft. Washington, Pa.). Biofilm growth was initiated as previously described (27) and processed for microscopy after growth for 16 to 18 h. Briefly, cells and biofilms were washed once in 10 mM phosphate-buffered saline (PBS), fixed at room temperature for 1 day in 2 ml of 3.7% formaldehyde in 10 mM PBS, and dehydrated through a series of ethanol rinses. *S. mutans* cells were then air dried on 0.08-μm-pore-diameter polyvinylidene difluoride (PVDF) filters (Poretics, Livermore, Calif.), or dried directly on Thermodox coverslips at critical point with liquid CO_2. All samples were sputter coated with a gold-palladium mixture and examined with a JSM-T300 scanning electron microscope (JEOL-Technics Co., Tokyo, Japan).

TABLE 2. Primers used in this study

Primer	DNA sequence (5′→8′)	Primer orientation
F20	GTAAAACGACGGCCAGT	Reverse
TnLO	GTGAAGTATCTTCCTAC	Forward
WWF.1	GATGTCCTCTACCCAT	Forward
WWR.1	GCTCTTCTCTAGTCCATG	Reverse
MBF.1	GAGGAGTATATGGCTAAGGAC	Forward
MBR.1	CACGGGCCAAAAGCTCTTCTC	Reverse
Tar-GS-Ent-F	GAGACGCCATTGAGTCAACTGAC	Forward
TarC-GS-For1	TGTGACTGGTCTTGATCGTGGAG	Forward
TarC-GS-Rev1	CGAATGATATACCCCATGCCG	Reverse
AF-gtfD-F	GCCTTAACGGACACTTCTC	Forward
AF-gtfD-R	GGAAGTCATAGCCACCAG	Reverse
GtfD-GS-For	CATTGCTGTCGCTTCTGGTTTG	Forward
GtfD-GS-Rev	GCCGCCTTATCATCCTCACTTTTC	Reverse
gbpC-RT-For	CCAACAACTCCTGATGAACCAACG	Forward
gbpC-RT-Rev	AGCAGCCCCAGTATGTGGAAG	Reverse
rpsL-For	CCAGTTGGTTCGTAAGCCAC	Forward
rpsL-Rev	GAGCAGAGTTAGGTTTCTTAGGG	Reverse

Bacterial transformation. *E. coli* was electrotransformed according to established protocols (37). Competence-stimulating peptide (CSP) (D.G.C., University of Toronto, Ontario, Canada) was used according to the protocol of Li et al. (24) for natural transformation of *S. mutans* UA130.

Southern blot. Chromosomal DNA isolated from *S. mutans* UA130 was digested and prepared for Southern blot analysis as previously described (41, 43). Plasmid pAM620 was radiolabeled with [α-^{32}P]dATP (3,000 Ci/mmol) (New England Nuclear) by nick translation (Gibco BRL) according to the recommendations of the supplier and used as a probe. Unincorporated radionucleotides were removed from the reaction mixture by Sephadex G-25 chromatography (5′-3′, Inc.).

Cloning the GMS315 transposon insertion site. The Tn*916*:*tar* junction fragment was cloned from the *S. mutans* chromosome as previously described (32). Briefly, 1 μg of chromosomal DNA from the nonadherent mutant (GMS315) and 1 μg of pUC19 DNA (Table 1) were digested with *Eco*RI. The enzyme was then heat inactivated at 65°C, and 100 to 200 ng of the chromosomal DNA was mixed with 60 to 120 μg of pUC19 in a final reaction volume of 10 μl for overnight ligation at 4°C according to the suggestions of the supplier (Promega). One microgram of the ligation mixture was then used for PCR amplification with TnLO and F-20 as primers (Table 2), which are specific for the 3′ end of the Tn*916* transposon and pUC19, respectively. A 100-μl reaction volume contained 2.0 mM $MgCl_2$, 20 mM Tris-HCl (pH 8.4), 50 mM KCl, 20 pmol of forward and reverse primers, and 1.0 μl of *Taq* polymerase (Promega). Amplification occurred in a thermal cycler (Hybaid, Ltd., Ashford, United Kingdom) for 35 cycles at 94°C for 30 s, 58°C for 30 s, and 72°C for 90 s. The 1.3-kb amplicon was subsequently TA cloned into pCR2.1 according to the suggestions of the supplier (Invitrogen) and introduced into electrocompetent *E. coli* DH5α. Transformants were selected on L agar plates supplemented with ampicillin, and plasmid DNA was isolated on Miniprep spin columns (Qiagen) and confirmed by Southern blotting and nucleotide sequence analysis.

Sequence analysis. Automated sequencing was performed at the nearby University of Vermont in an ABI 373XC automated sequencing machine. The EMBL and GenBank databases were searched for similar sequences by using the FASTA format, and sequence analysis was performed with MacDNAsis version 2.0 software. Open reading frames flanking the transposon insertion in GMS315 were identified upon in silico analysis of the *S. mutans* genome (http://www.genome.ou.edu/smutans.html). Alignments were generated and analyzed with the ClustalW server available through the European Bioinformatics Institute at http://www.ebi.ac.uk/clustalw/. Primers were designed and analyzed with MacVector 7.0 software (Oxford Molecular).

Cloning and disruption of *S. mutans tarC*. A 0.93-kb amplicon containing the *tarC* gene was PCR amplified from the *S. mutans* UA130 chromosome using WW.F.1 and WW.R.1 as primers (Table 2). The amplicon was subsequently cloned into the pGEMT-Easy TA cloning vector (Promega), and the resulting pMB12 construct (Table 1) was confirmed by restriction enzyme mapping and Southern blot analysis. A kanamycin resistance cassette (ΩKm) (36) isolated from plasmid pUC4ΩKm upon digestion with *Eco*RI was then ligated into the unique *Mfe*I site within the cloned *tarC* coding sequence, and the resulting construct, pKO (Table 1), was further digested with *Pvu*I to disrupt the β-lactamase gene resident on the plasmid. The resulting pRG.2 recombinant construct was electrotransformed into *E. coli* DH5α and confirmed by restriction enzyme mapping and Southern blot analysis. Plasmid pRG.2 was linearized and then used to transform *S. mutans* UA130 with CSP according to the protocol of Li et al. (24). To select for the double-crossover event, chromosomal DNA was isolated from *S. mutans* transformants demonstrating resistance to kanamycin as previously described, digested with *Mun*I (New England Biolabs), and resolved (6 μg per lane) on 0.8% agarose gels for subsequent transfer to nitrocellulose by Southern blotting. A 480-bp probe that is internal to the *tarC* coding sequence was PCR amplified from the *S. mutans* chromosome under the conditions described above with primers MBF.1 and MBR.1 (Table 2). The probe was nick translated, and the nitrocellulose membranes were hybridized and washed as described for the Southern blot.

Phenotypic characterization of *S. mutans*. Bacterial cells from *S. mutans* overnight cultures were serially diluted and plated onto mitis salivarius (MS) agar (Acumedia) for incubation at 37°C and 5% CO_2. Following incubation for 16 to 18 h, the colonial morphologies were documented by photography through an Olympus dissecting microscope. To visualize *S. mutans* cell arrangements, cells from overnight cultures grown in the presence of 1% sucrose were heat fixed to glass slides and stained with crystal violet for examination with an Olympus CX40 light microscope at ×1,000 under oil immersion. Fields were selected at random for photography.

RNA isolation. Total RNA was isolated from *S. mutans* cultures for subsequent Northern blot, reverse transcription-PCR (RT-PCR), and real-time RT-PCR experiments using a modification of the Fast RNA BLUE kit protocol (BIO 101). First, bacterial cell aggregates were disrupted in a sonicating water bath (Braun) for 20 s. The cells were then lysed mechanically in the presence of ceramic beads at a setting of 6 in a Fast Prep machine (BIO 101) for 33 s, and the RNA was purified via a series of Trizol and Trizol-chloroform (3:1) extractions followed by alcohol precipitation. The RNA was checked for integrity on a 1.2% agarose gel, after which it was treated with RQ1 RNase-free DNase (Promega) according to the recommendations of the supplier. Total RNA was quantitated in a Genosys spectrophotometer (Fisher Biotech) according to the optical density at 600 nm (OD_{600}) (1 OD_{600} unit = 40 μg/ml).

RT-PCR. RT-PCR was used to characterize transcription of the *S. mutans tarC* gene. Specifically, a first-strand cDNA synthesis kit (MBI Fermentas, Burlington, Ontario, Canada) was used to amplify 1 μg of DNase-treated total RNA isolated from cultures grown in THB. Random hexamers (0.2 μg), RNase inhibitor (20 U), deoxynucleoside triphosphates (dNTPs [10 mM]), and Moloney murine leukemia virus (M-MuLV) reverse transcriptase (20 U/μl) were added to the reaction mixture, which was incubated at 25°C for 15 min and then at 37°C for 1 h in accordance with the recommendations of the supplier. Second-strand cDNA synthesis was performed with the *tar*-spanning primers TarC-GS-Ent-F and TarC-GS-Rev1, which anneal to the 5′ and 3′ ends of ORF1 and *tarC*, respectively, as well as with primers TarC-GS-For1 and TarC-GS-Rev1, which are internal to the *tarC* coding region (Table 2). The primers were added to each reaction mixture at a final concentration of 2.5 μM, and the reaction mixtures were subjected to PCR amplification with an annealing temperature of 53°C for a total of 35 cycles in a Hybaid thermocycler (Hybaid Ltd.). Ten microliters of each amplified product was analyzed on a 1% agarose gel containing 0.5 μg of ethidium bromide per ml.

Northern blotting. Northern hybridization experiments were performed as previously described (42). *S. mutans gtfD*-specific probes were PCR amplified from the UA130 chromosome with primers AF-gtfS-F and AF-gtfS-R (Table 2) and then radiolabeled with [α-^{32}P]dATP (3,000 Ci/mmol) (New England Nuclear) by using a nick translation kit (Gibco BRL). Unincorporated radionucleotides were removed from the reaction mixture by Sephadex G-25 chromatography (5′-3′, Inc.). The blots were hybridized overnight in a Lab-line hybridization oven at 42°C with gentle agitation in ULTRAHyb hybridization buffer (Ambion) and washed in accordance with the recommendations of the supplier. The blots were then air dried and exposed to X-ray film (Kodak Biomax ML) for 24 h at −80°C in the presence of an intensifying screen prior to autoradiography.

Real-time quantitative RT-PCR. Single-stranded cDNA, synthesized from total RNA as described above for RT-PCR, was amplified in a QuantiTect SYBR Green PCR Master Mix (Qiagen) containing dNTPs, HotStarTaq DNA polymerase, SYBR Green I, ROX (a passive reference dye), and 5 mM $MgCl_2$. Each PCR mixture contained 100 ng of template cDNA, 1× Master Mix, and 250 nM (each) GtfD-GS-For/GtfD-GS-Rev or gbpC-RT-For/gpbC-RT-Rev primer (Table 2). Amplification was performed in a Cepheid Smart Cycler (Cepheid, Sunnyvale, Calif.) according to the following thermal cycling protocol: 95°C for 15 min for initial denaturation, followed by 40 cycles of three steps consisting of 94°C for

15 s, 54°C for 30 s, and 72°C for 30 s. Standard curves were generated for each primer-template set with a series of *S. mutans* UA130 genomic DNAs diluted 10-fold and then used to calculate correlation coefficients and to translate concentration threshold (Ct) values into relative DNA copy number. The Ct was defined as the cycle at which SYBR green fluorescence was detected at a level above background. Quantification of *gtfD* and *gbpC* cDNA was normalized to the amount of cDNA derived from a ribosomal protein (*rpsL*) control, the expression of which does not vary under the experimental test conditions.

Protein isolation. *S. mutans* cultures grown to the mid-logarithmic phase (OD_{600} = 0.4 to 0.6) were pelleted for 5 min at 4,300 × *g* in an SS-34 rotor, washed once in 10 ml of PBS, and resuspended in 500 μl of PBS supplemented with protease inhibitor cocktail (Boehringer Mannheim). Cells were disrupted at 4°C for three intervals of 60 s each in a Mini-Bead Beater (BioSpec) using 0.1-mm-diameter zirconium beads, and the resulting cell lysates were cleared by centrifugation at high speed in an Eppendorf Microfuge for 30 s.

For Western blot analysis, secreted proteins were precipitated from culture supernatants upon treatment with 50% trichloroacetic acid (TCA) for 30 min at 4°C. The precipitated proteins were harvested by centrifugation at 12,000 × *g* for 15 min in an SS-34 rotor at 4°C and resuspended in 300 to 500 μl of 0.1 M Tris-base supplemented with a protease inhibitor cocktail (Boehringer Mannheim). Protein determinations were defined with a Pierce bicinchoninic acid (BCA) assay kit (Bio-Rad) using bovine serum albumin as a standard.

SDS-PAGE. *S. mutans* proteins (100 μg per lane) were resolved on a denaturing SDS-PAGE (5 to 10% polyacrylamide) gradient gel by electrophoresis, and the gels were subsequently stained with 0.1% Coomassie blue (Sigma). Proteins run in parallel on duplicate gels were not stained but rather electrophoretically transferred overnight to polyvinylidene difluoride (PVDF) or nitrocellulose membranes in a Hoefer apparatus at 0.2 A and 4°C for N-terminal sequencing or immunoblotting, respectively.

N-terminal sequencing. Protein sequence determination was performed on a fee-for-service basis at the University of Texas Medical Branch at Galveston. An Applied Biosystems 475A protein sequencing system equipped with a blot cartridge was used to perform Edman degradation.

Immunoblotting. Membranes were blocked overnight in 5% nonfat dry milk in Tris-buffered saline (TBS) (2.42 g of Tris per liter, 8 g of NaCl per liter, 0.38% 1 N HCl) and with gentle shaking. Washes were performed at 25°C in TBS with 0.1% Tween 20 (TBST). A polyclonal anti-Gtf-S antiserum (gift of Howard Kuramitsu, SUNY, Buffalo, N.Y.) was applied to the membrane at a dilution of 1:5,000 in TBST, and the secondary peroxidase-conjugated goat anti-rabbit antibody (Pierce) was used at a 1:10,000 dilution. Enhanced chemiluminescence was performed according to the recommendations of the supplier (Amersham) and visualized on Kodak X-Omat (XAR-4) film.

Assessment of the cariogenic potential of *S. mutans* GMS315 and GMS900 in germfree rats. Three groups of seven germfree Fisher rats each were challenged with oral swabs saturated with 10^8 CFU of *S. mutans* UA130, GMS315, or GMS900 per ml as previously described (29). Over the next 3 days, the rats were challenged repeatedly with fresh swabs of the appropriate strain, and on the 8th day postchallenge, swab samples were collected and plated onto blood agar and MS agar plates to confirm colonization. This procedure was repeated once again 14 days postchallenge. All rats were provided water ad libitum supplemented with antibiotic when appropriate and maintained on caries-promoting diet 305, also provided ad libitum (29). Forty-five days postchallenge, the rats were sacrificed, and their mandibles were removed. Plaque microbiology was performed on one mandible from each animal and subsequently processed for caries scores (17). Data were analyzed by using the Mann-Whitney U test, and differences were considered to be significant when $P < 0.05$.

RESULTS

Identification and characterization of an *S. mutans* adherence mutant. We screened an *S. mutans* Tn*916* transposon library for mutants altered in their ability to adhere to borosilicate glass tubes when grown in THB and 1% sucrose. One mutant, GMS315, proved to be adherence deficient in this in vitro model of the tooth surface (Fig. 1A). The results of saliva-coated hydroxyapatite assays also indicate that *S. mutans* GMS315 is significantly less adherent than the wild type: $(4.8 \pm 3.5) \times 10^8$ CFU recovered from GMS315 supernatants versus $(2.9 \pm 1.1) \times 10^7$ CFU from UA130 supernatants ($P < 0.05$). Importantly, Southern blots of GMS315 chromosomal DNA restricted with *Hin*dIII (which cuts once within the transposon) and probed with radiolabeled pAM620 revealed only two *Hin*dIII junction fragments, consistent with a single transposon insertion in the chromosome (data not shown).

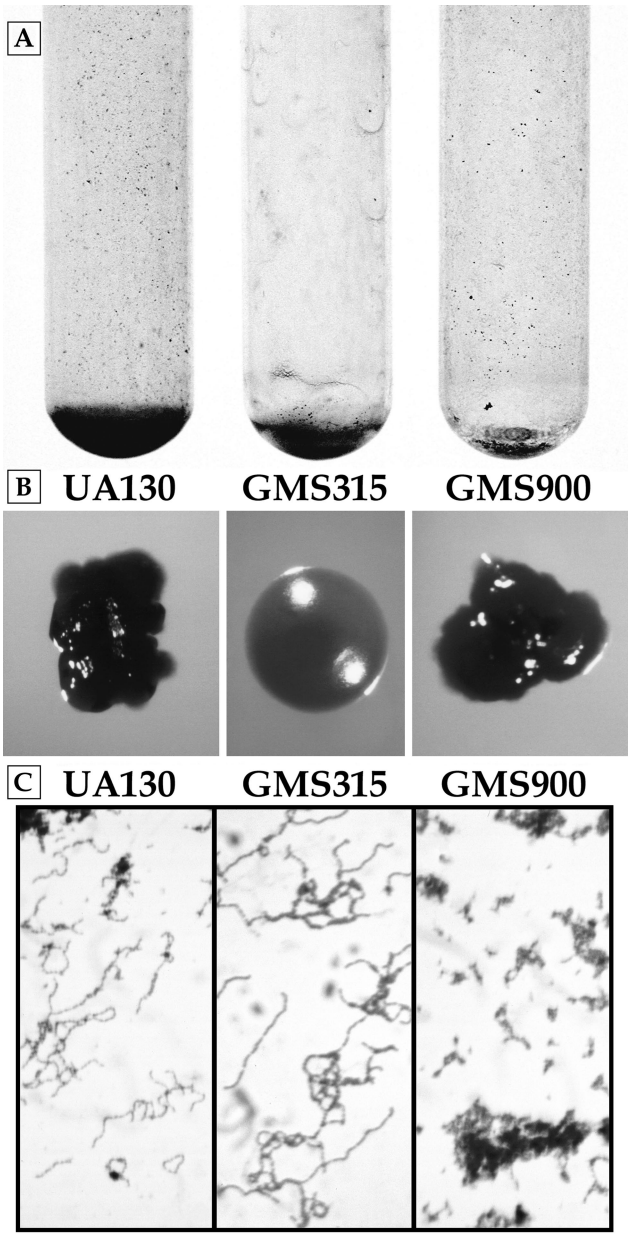

FIG. 1. Phenotypic analysis of *S. mutans* UA130 and isogenic mutants GMS315 and GMS900. (A) Adherence assay. *S. mutans* UA130 cells stained with crystal violet are adherent to the surfaces of borosilicate glass tubes, whereas GMS315 cells are not. Also noteworthy is the adherence of GMS900 cells to glass, which is notably compromised relative to that of the UA130 progenitor. (B) Colonial morphology. GMS315 grown on MS agar displays a smooth colonial morphology typical of nonadherers. In contrast, GMS900 and UA130 colonies are rough with raised centers. (C) Microscopy. *S. mutans* UA130 and isogenic mutant GMS315 grown in THB assume typical chain-like arrangements. In contrast, aggregates of chains are evident in GMS900 cultures grown in this medium.

The colonial morphology of *S. mutans* GMS315 differed

significantly from that of UA130 when grown on MS agar (Fig. 1B). GMS315 colonies presented with a smooth and glossy phenotype typical of nonadherers, whereas UA130 exhibited rough colonies with raised centers. The growth of UA130 and GMS315 in liquid culture was homogeneously distributed throughout the culture medium, and light microscopy confirmed typical chain-like arrangements consisting of 8 to 12 cells (Fig. 1C).

SEM of *S. mutans* UA130 and GMS315 whole cells. We prepared scanning electron micrographs of *S. mutans* cells grown to the mid-logarithmic phase in THB supplemented with 1% sucrose to more closely examine the surface properties of the GMS315 adherence-deficient mutant and its UA130 wild-type progenitor. Interestingly, SEM revealed what appears to be the release of a significant amount of capsular polysaccharide from the surface of GMS315 (Fig. 2A). This phenomenon was hardly evident in the wild-type strain.

GMS315 lacks a 155-kDa protein. Protein profiles for *S. mutans* UA130 and GMS315 resolved on SDS-PAGE gels revealed a missing 155-kDa species from GMS315 that was present in UA130 (Fig. 3). Western blot analysis revealed reactivity of the 155-kDa protein with a polyclonal anti-Gtf-S antiserum, and subsequent N-terminal sequencing of the protein confirmed its identity as Gtf-S, a glucosyltransferase encoded by *gtfD* that is responsible for the synthesis of water-soluble glucans (10). A 130-kDa protein present in UA130 but absent from GMS315 also reacts with the anti-Gtf-S antiserum and likely represents a second form of Gtf-S derived from degradation of the parental 155-kDa protein by endogenous proteases. Similar findings have been reported for *S. gordonii*, in which the native 174-kDa Gtf-S species was accompanied by a lower-molecular-mass form of Gtf-S on activity gels and Western blots (46).

Characterization of the *S. mutans tar* locus. We mapped the unique Tn*916* insertion in *S. mutans* GMS315 and identified the insertion site upon in silico analysis of the completed *S. mutans* UA159 genome. Our analysis revealed insertion of the transposon 288 bp upstream of an ORF that we call "*tarC*," previously designated *gcrR* in accordance with its proposed role as a regulator of GbpC expression (39) (Fig. 4A). The *tarC* gene was located at bp 1804158 to 1803470 in the *S. mutans* genome database, encoding a hypothetical protein of 229 amino acids with a predicted molecular mass of 25,190 Da. The results of RT-PCR experiments confirm that *tarC* transcription is independent of ORF1 and is driven by a *tarC*-specific promoter that is likely located between ORF2 and TarC (Fig. 4B). Sequence analysis with the BLASTP program (1) revealed up to 91% shared amino acid identity between TarC and other DNA-binding bacterial response regulators, such as CsrR in *Streptococcus pyogenes* (23) and Llr in *Lactococcus lactis* (34) (Fig. 5). In addition, TarC harbors an aspartate residue that is strictly conserved at amino acid position 54 in other response regulators and represents the putative site of phosphorylation. Interestingly, the *tarC* sequence does not align with any of the 13 proposed two-component signal transduction systems in the *S. mutans* genome, but rather represents one of five putative orphan response regulators on the chromosome.

Confirmation and characterization of *S. mutans* GMS900, a *tarC* knockout mutant. To assess the putative effect(s) of the TarC response regulator on *S. mutans* plaque formation and cariogenesis, we cloned the *tarC* coding sequence and disrupted it with a kanamycin resistance cassette (ΩKm) before returning it to the *S. mutans* UA130 chromosome by allelic exchange. The double-crossover event was confirmed by PCR and Southern blot analysis (data not shown). Interestingly,

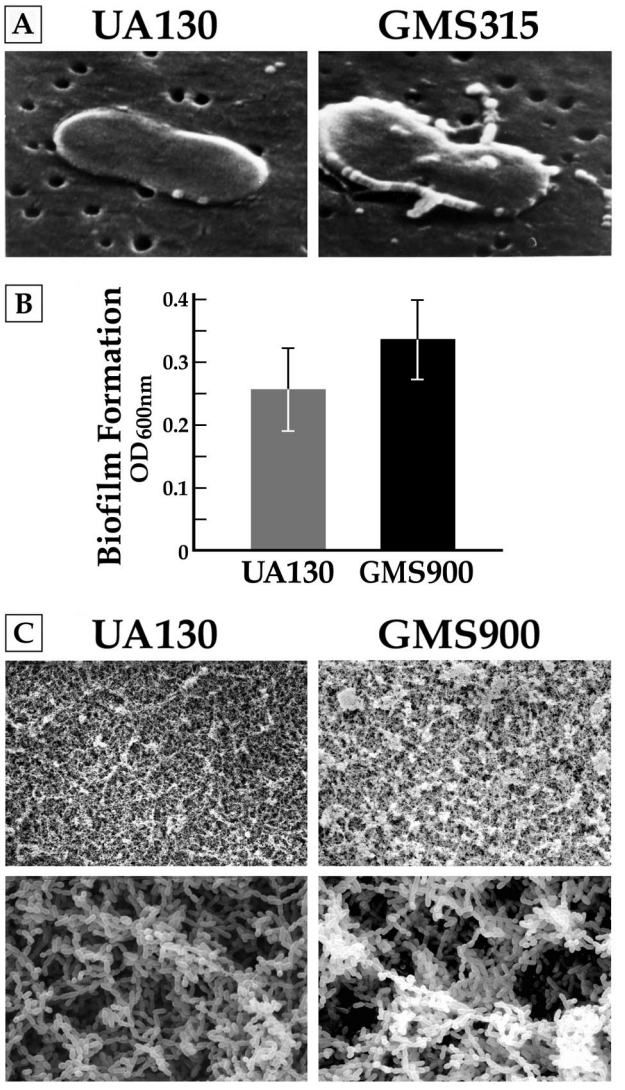

FIG. 2. Scanning electron micrographs. (A) Exponential-phase cultures of *S. mutans* UA130 and GMS315 were grown in THB supplemented with 1% sucrose and air dried onto Poretic PVDF filter membranes. The release of capsular polysaccharides from GMS315 is more prevalent than from the UA130 wild-type progenitor. Images were obtained at a magnification of ×61,000. (B) *S. mutans* UA130 and GMS900 biofilms were quantified in an established microtiter assay (2). Numbers of plaque organisms in UA130 and GMS900 biofilms after formation for 16 h on polystyrene Thermonox coverslips were not significantly different, ruling out the possibility that differences in biofilm architecture are due to differences in biomass. (C) GMS900 exhibits a biofilm architecture that is different from that of the wild type. Specifically, GMS900 forms many more cellular aggregates than the wild type, which are clearly visible at magnifications of both ×500 (top) and ×5,000 (bottom). Moreover, streptococcal chain length appears to be greater in GMS900 (10 to 15 cells) than in the wild type (5 to 10 cells), with fewer diploid cells in the latter.

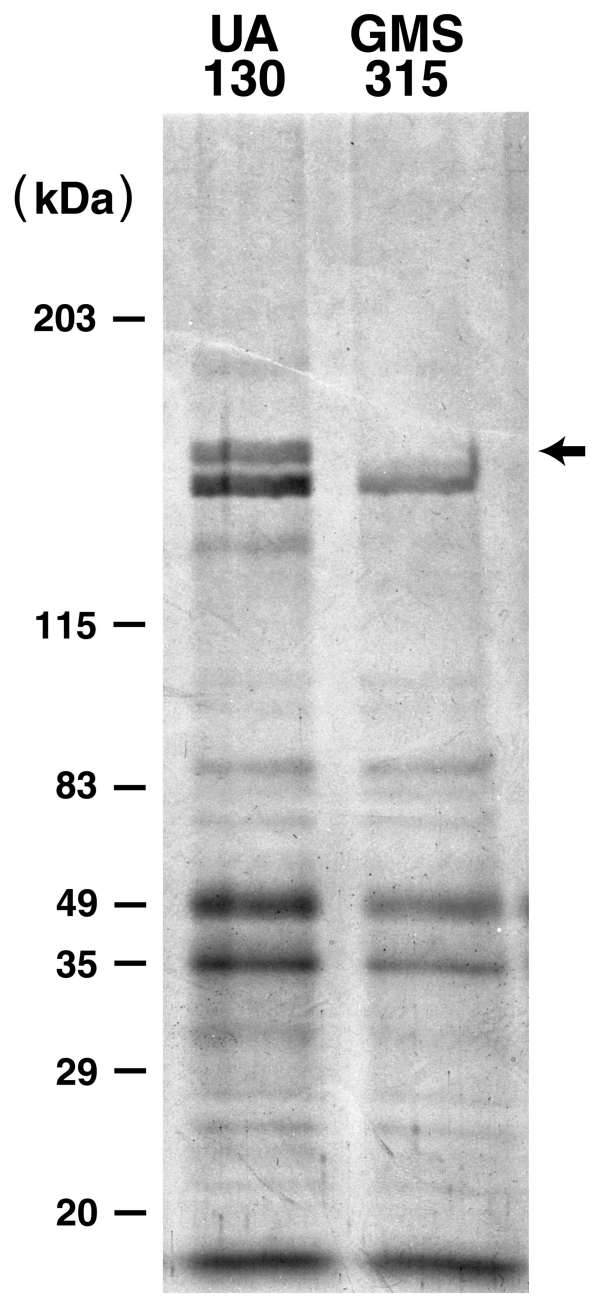

FIG. 3. *S. mutans* protein profiles. Coomassie blue-stained gel of *S. mutans* whole-cell lysates reveals a 155-kDa protein that is present in UA130 but missing from the GMS315 transposon mutant (arrow). Immunoblotting and N-terminal sequence analysis confirmed that the missing protein is Gtf-S. A 130-kDa protein that is present in UA130 but absent from GMS315 also reacts with the anti-Gtf-S antiserum and likely represents a second form of Gtf-S deriving from proteolytic degradation of the parental protein.

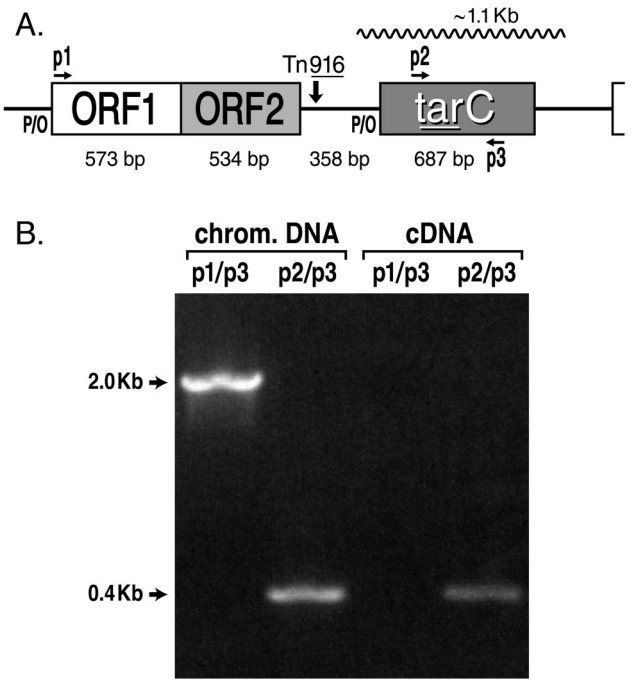

FIG. 4. Structural organization of the *S. mutans tar* locus. (A) The results of RT-PCR experiments support transcription of *tarC* from a promoter (P/O) located immediately upstream. Putative −10 and −35 promoter sequences are present in this noncoding region, as well as a ribosome binding site upstream of the TarC translation start codon. The solid arrows indicate the primers used for RT-PCR. (B) Gel electrophoresis of amplified DNA fragments derived from the *S. mutans* chromosome or cDNA templates. Lane designations p1/p3 and p2/p3 represent the primer pairs used in the amplification.

GMS900 was significantly compromised in its ability to adhere to borosilicate glass (Fig. 1A) and saliva-coated hydroxyapatite compared to that of the wild type, and it was unique in that it formed large cellular aggregates that settled to the bottom of the tube when grown in liquid culture. Indeed, extensive cell clumping was also evident upon microscopic analysis of GMS900 in liquid culture (Fig. 1C), despite a colonial morphology that approximated that of the wild type on MS agar (Fig. 1B). Also noteworthy is that GMS900 biofilms that formed on polystyrene disks could be more readily dislodged from the surface than those formed by the UA130 wild-type strain.

SEM of *S. mutans* biofilms. Closer examination of *S. mutans* biofilms by SEM revealed a plaque architecture for GMS900 that was notably different from that of the wild type, although the total biomasses for GMS900 and UA130 biofilms were similar, as determined by crystal violet release assays (Fig. 2B). Specifically, the mutant biofilm formed many large aggregates of cells and took on a "patchy" appearance due to large areas that were devoid of cells (Fig. 2C). Under higher magnification, we noted that approximately 25% of GMS900 cells were arranged in chains 10 to 15 cells long, and 75% of the cells appeared diploid. In contrast, nearly 50% of the UA130 cells were arranged in shorter chains of 5 to 10 cocci, and only 50% of the cells appeared to be diploid.

***S. mutans tarC* mutants are hypocariogenic in germfree rats.** To determine whether alterations in *S. mutans* biofilm architecture affects cariogenesis, we mono-infected germfree rats with GMS315, GMS900, or the UA130 wild-type progenitor. The rats were maintained on a sucrose-containing, caries-pro-

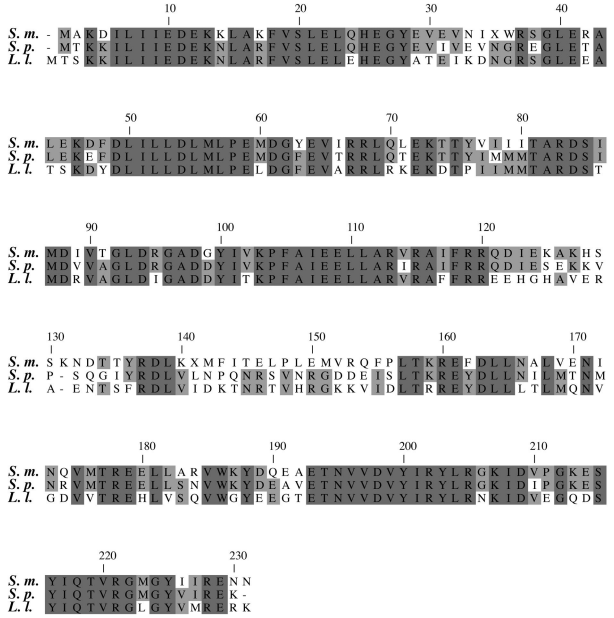

FIG. 5. *S. mutans* TarC alignment. Alignment of the *S. mutans* (*S.m.*) TarC sequence with CsrR and Llra response regulator sequences from *Streptococcus pyogenes* (*S.p.*) and *Lactobacillus lactis* (*L.l.*). The conserved aspartate residue at position 54 represents the putative site of phosphoryl transfer. Darkly shaded boxes denote regions of amino acid identity that are conserved across all three bacterial species. Lighter-shaded boxes represent shared amino acid identity across two bacterial species.

moting diet for 45 days postinoculation, after which plaque microbiology and caries scores were obtained for each mandible. The results of these studies revealed that both mutants were compromised in their ability to colonize rat molars, and they caused significantly fewer cavities on the buccal and sulcal surfaces of teeth than wild-type (Table 3).

Regulation of *S. mutans* Gtf-S and GbpC expression. To examine the relative abundance of *gtfD*- and *gbpC*-specific mRNAs in *S. mutans* UA130, GMS315, and GMS900, we performed Northern hybridization and/or real-time RT-PCR experiments. Northern blot analysis revealed a 3.8-kb *gtfD*-specific transcript that was more abundantly expressed in GMS900 than in either GMS315 or UA130 (data not shown). The results of quantitative chemiluminescent Western blots further validate these expression patterns by revealing levels of total Gtf-S that are elevated in GMS900 and diminished in GMS315 relative to the wild type (Fig. 6). The localization of Gtf-S to the pellet fraction of GMS900 versus culture supernatants of GMS315 is also evident on these immunoblots. Finally, the results of real-time RT-PCR revealed increased *gtfD* expression in the GMS900 *tarC* knockout mutant (mean Ct = 28.25 for GMS900 and 30.80 for UA130; $n = 3$) relative to that in the wild type (Fig. 7). Likewise, *gbpC* expression was increased in GMS900 relative to that in the wild type (mean Ct = 24.60 for GMS900 and 29.30 for UA130; $n = 3$). Taken collectively, these results indicate a near-fivefold increase in *gtfD* and *gbpC* expression in the GMS900 TarC knockout mutant relative to the wild type.

TABLE 3. Colonization and cariogenic potential of *S. mutans* UA130 and isogenic mutants GMS315 and GMS900 in germfree rats

S. mutans strain	Colonization (10^5 CFU)[a]	Total caries score[b]
Comparison 1		
UA130 (wild type)	228.6 ± 91.7	96 ± 26
GMS315	121.4 ± 42.5	75 ± 29[c]
Comparison 2		
UA130 (wild type)	16.4 ± 8.8	106 ± 27
GMS900	4.0 ± 1.5	99 ± 19[c]

[a] Values represent the mean ± the standard deviation for 7 rats per group.
[b] Values represent the median ± the range for 7 rats per group. Results for buccal and sulcal carious lesions were similar.
[c] Significantly different ($P < 0.025$) from the respective UA130 wild type sample as determined by the Mann-Whitney U test.

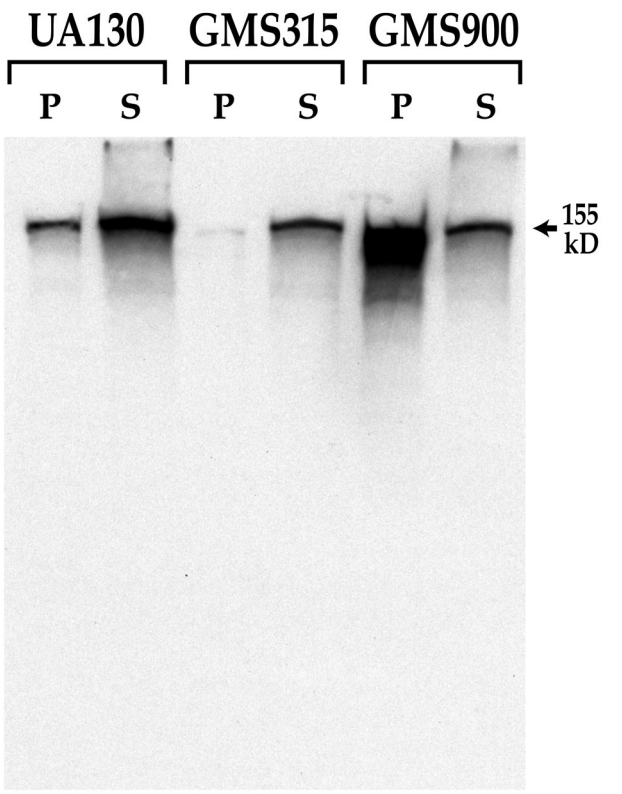

FIG. 6. Gtf-S expression in *S. mutans* cell pellets versus culture supernatants. Shown is a Western blot of *S. mutans* UA130, GMS315, and GMS900 proteins from pellet (P) or culture supernatant (S) fractions that react with a polyclonal rabbit anti-Gtf-S antiserum. Total expression (P+S) of the 155-kDa Gtf-S protein (arrow) is decreased in GMS315 but increased in GMS900 relative to that in the wild type. Moreover, Gtf-S predominates in the pellet fraction of GMS900 versus the culture supernatants of UA130 and GMS315.

DISCUSSION

In the present study, we characterized two *S. mutans* mutants, GMS315 and GMS900, as poor colonizers of the tooth surface and as significantly hypocariogenic in a germfree rat model. Both mutants harbor mutations near or within the *tarC*

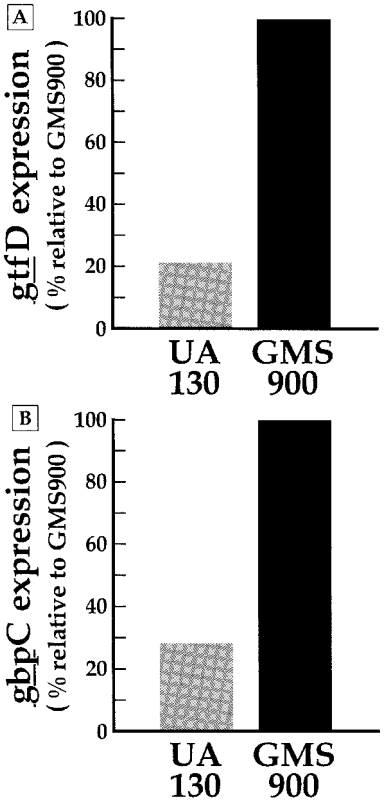

FIG. 7. Effect of TarC on *S. mutans gtfD* expression. Expression of *gtfD* (A) and *gbpC* (B) was quantified in UA130 and GMS900 cell samples by real-time RT-PCR. The concentration thresholds for each sample were defined and applied to standard curves obtained during the same experiment. Shown for *gtfD* and *gbpC* are the results of a single representative experiment from a total of three independent experiments. The results, which have been normalized to cDNAs derived from an *rpsL* control and expressed as percent relative to GMS900, indicate that the levels of *S. mutans gtfD* and *gbpC* expression are nearly fivefold higher in GMS900 than in the wild type.

gene, the product of which shares extensive homology with other bacterial response regulators. The results of Northern blotting and real-time RT-PCR assays revealed significantly increased *gtfD* and *gbpC* expression in the GMS900 *tarC* knockout mutant relative to the wild type, supporting TarC as a negative transcriptional regulator of these sucrose-dependent activities. We propose that the smooth colonial morphology of the *S. mutans* GMS315 transposon mutant reflects the release of glucans noted on scanning electron micrographs (Fig. 2A) and that a transposon-borne promoter (4) favors TarC accumulation and decreased transcription of *gtfD* and/or *gbpC* in this mutant. The results of Northern hybridization experiments conducted in our laboratory support down-regulation of *gtfD* in GMS315 (data not shown).

Until recently, the contribution of Gtf-S to *S. mutans* adherence was unclear, although it had been reported that Gtf-S-deficient mutants of *S. mutans* demonstrated reduced smooth surface caries in vivo (47). In a report by Vickerman and Clewell, increased GtfG expression in *S. gordonii* had no effect on initial levels of adherence to saliva-coated hydroxyapatite, but did have a profound effect on sucrose-dependent attachment and accumulation (46). Our findings are consistent with this report and support a role for Gtf-S in *S. mutans* sucrose-dependent adherence, plaque formation, and caries development. Specifically, we propose that increased *gtfD* expression in the GMS900 TarC knockout mutant shifts glucan production to favor a significantly higher proportion of α1,6 glucans. In turn, these water-soluble polymers may provide *S. mutans* GbpC, a glucan-binding lectin (38), with more binding substrate and so promote α1,6 glucan-dependent aggregation. The results of quantitative Western blot analysis conducted in our laboratory support this hypothesis by revealing less Gtf-S in GMS900 culture supernatants than in the UA130 wild-type progenitor strain and more Gtf-S in the GMS900 cell-associated fraction than in the wild type. Also consistent with this hypothesis are the results of real-time RT-PCR experiments that reveal increased GtfD and GbpC expression in GMS900. Interestingly, we characterized *S. mutans* GMS900 as an aggregating mutant and report that it is compromised in sucrose-dependent adherence to in vitro models of the tooth surface and to rat molars. These findings are consistent with those from other aggregating mutants of *S. mutans*, like GMS900, that are poor adherers and do not accumulate well on hydroxyapatite beads (45).

The mechanism by which inactivation of TarC affects *S. mutans* biofilm formation and subsequent caries formation is not entirely clear. Dental plaque is a biofilm of adherent bacterial cells separated by fluid-filled spaces and imbedded in a capsular polysaccharide matrix, and the involvement of multiple *S. mutans* genes in its formation has been confirmed (2, 3, 12, 48). The present study is the first to specifically implicate *gtfD* and *gbpC* transcription in *S. mutans* biofilm formation, since derepression of these genes in a TarC knockout mutant results in an aberrant biofilm comprised of numerous cell aggregates situated around what appear to be enlarged water channels (Fig. 2C). Interestingly, reports by Ooshima et al. (35) describe an optimal GtfB/GtfC/GtfD ratio of 20:1:4 as necessary for appropriate colonization in vitro, and hence deviations from this ratio could compromise the adherence properties and structure of the plaque biofilm. In addition to poor attachment of the GMS900 mutant biofilm to a solid substratum, we also noted alterations in its plaque structure that include an increase in streptococcal chain length. We believe such a change in architecture could compromise the diffusion barrier that is established by the biofilm at the tooth surface and so reduce the acidogenic potential of *S. mutans* in the plaque environment. Moreover, the transport of nutrients and waste products into and out of the plaque biofilm via enlarged water channels may further attenuate *S. mutans*-induced cariogenesis. Future work will investigate acid tolerance and substrate transport (including antibiotics) in UA130 and GMS900 biofilms to elucidate these and possibly other functional consequences of altered biofilm architecture.

Accumulating evidence in the literature supports a role for signal transduction in regulation of bacterial biofilm development and pathogenesis (2, 7, 13, 16, 20, 27, 49). Gtf-S, which facilitates sucrose-dependent adherence of *S. mutans*, and GbpC, which promotes the cohesive properties of the plaque biofilm through synthesis and binding of a polysaccharide matrix, are both proteins with activities that warrant fine-tuned regulatory control to optimize appropriate biofilm and caries formation. Experiments aimed at examining *S. mutans* gene

expression in response to a variety of environmental signals, such as nutrient availability, oxygen content, and pH changes, could elucidate a specific role for the TarC response regulator in signal transduction, formation of the plaque biofilm, and disease. Typical signal transduction systems are comprised of a transmembranous histidine kinase (HK) and a cytosolic response regulator. HKs are sensors that bind an extracellular signaling ligand, which in gram-positive bacteria is often a peptide pheromone (6, 18), and become autophosphorylated at a histidine residue located near the carboxyl terminus of the protein. The phosphate is then transferred to an acidic aspartate residue that is highly conserved at amino acid position 54 on the cognate response regulator. Such His-Asp signal propagation activates the response regulator to bind DNA and exert its effect or effects on the transcription of targeted genes.

HKs and response regulators that belong to a common two-component signaling pathway are often encoded by genes that are organized as an operon on the bacterial chromosome (14). TarC is unlike other response regulators, however, in that it shares no apparent association with a cognate HK. This is indicated by RT-PCR analysis, which reveals a single monocistronic mRNA that is derived from a promoter located immediately upstream of *tarC*. While it is unclear how orphan response regulators like TarC modulate gene expression, one could envision their involvement as intermediaries of in vivo cross talk between otherwise independent signal transduction systems. In fact, a recent report in the literature supports phosphoryl transfer from a sensory kinase to a noncognate response regulator in *E. coli* (44), and cross talk has been suggested in the regulation of *S. mutans* acid tolerance by Li and coworkers (25).

In summary, this work is the first to report on the regulation of *S. mutans* glucan production and binding and how it modulates formation of the plaque biofilm and subsequent cariogenesis. It is possible that the TarC response regulator controls the expression of multiple *S. mutans* genes in response to an environmental signal. Future studies will include differential display PCR and two-dimensional gel electrophoresis approaches to reveal additional *S. mutans* genes that are subject to TarC control. Experiments are also planned to identify the signals to which the TarC regulator responds. Taken together, these investigations will promote our understanding of mechanisms of gene regulation and signal transduction in *S. mutans*, and facilitate the development of therapeutic approaches aimed at controlling formation of the plaque biofilm and subsequent cariogenesis.

ACKNOWLEDGMENTS

This work was supported by Public Health Service grant DE12246 to G.S. from the National Institute of Dental and Craniofacial Research, as well as by grants from the Sigma Xi Scientific Research Society, the Vermont Genetics Network (NCRR, 1 P20 RR16462), and the Middlebury College Department of Biology.

Special thanks go to Howard Kuramitsu for providing the anti-Gtf-S rabbit antiserum, Jan Novak for assistance with *tarC* cloning, Michelle von Turkovitch for expertise with SEM, Dilani Senadheera for help with real-time RT-PCR, and Gary Nelson for figure preparation.

REFERENCES

1. **Altschul, S. F., W. Gish, W. Miller, E. W. Myers, and D. J. Lipman.** 1990. Basic local alignment search tool. J. Mol. Biol. **215:**403–410.
2. **Bhagwat, S. P., J. Nary, and R. A. Burne.** 2001. Effects of mutating putative two-component systems on biofilm formation by *Streptococcus mutans* UA159. FEMS Microbiol. Lett. **205:**225–230.
3. **Burne, R. A., Y.-Y. M. Chen, and J. E. C. Penders.** 1997. Analysis of gene expression in *Streptococcus mutans* in biofilms *in vitro*. Adv. Dent. Res. **11:**100–109.
4. **Clewell, D. B., S. E. Flannagan, Y. Ike, J. M. Jones, and C. Gawron-Burke.** 1988. Sequence analysis of termini of conjugative transposon Tn*916*. J. Bacteriol. **170:**3046–3052.
5. **Costerton, J. W., Z. Lewandowski, D. E. Caldwell, D. R. Korber, and H. M. Lappin-Scott.** 1995. Microbial biofilms. Annu. Rev. Microbiol. **49:**711–745.
6. **Dunny, G. M., and B. A. Leonard.** 1997. Cell-cell communication in Gram-positive bacteria. Annu. Rev. Microbiol. **51:**527–564.
7. **Federle, M., K. S. McIver, and J. R. Scott.** 1999. A response regulator that represses transcription of several virulence operons in the group A streptococcus. J. Bacteriol. **181:**3649–3657.
8. **Haas, W., and J. Banas.** 2000. Ligand-binding properties of the carboxyl-terminal repeat domain of the *Streptococcus mutans* glucan-binding protein A. J. Bacteriol. **182:**728–733.
9. **Hamada, S., and H. D. Slade.** 1980. Biology, immunology, and cariogenicity of *Streptococcus mutans*. Microbiol. Rev. **44:**331–384.
10. **Hanada, N., and H. K. Kuramitsu.** 1989. Isolation and characterization of the *Streptococcus mutans gtfD* gene, coding for primer-dependent glucan synthesis. Infect. Immun. **57:**2079–2085.
11. **Hazlett, K. R. O., S. M. Michalek, and J. A. Banas.** 1998. Inactivation of the *gbpA* gene of *Streptococcus mutans* increases virulence and promotes in vivo accumulation of recombination between the glucosyltransferase B and C genes. Infect. Immun. **66:**2180–2185.
12. **Hazlett, K. R. O., J. E. Mazurkiewicz, and J. A. Banas.** 1999. Inactivation of the *gbpA* gene of *Streptococcus mutans* alters structural and functional aspects of plaque biofilm which are compensated by recombination of the *gtfB* and *gtfC* genes. Infect. Immun. **67:**3909–3914.
13. **Heath, A., V. J. DiRita, N. L. Barg, and N. C. Engleberg.** 1999. A two-component regulatory system, CsrR-CsrS, represses expression of three *Streptococcus pyogenes* virulence factors, hyaluronic acid capsule, streptolysin S, and pyrogenic exotoxin B. Infect. Immun. **67:**5298–5305.
14. **Hoch, J. A., and T. J. Silhavy (ed.).** 1995. Two-component signal transduction. ASM Press, Washington, D.C.
15. **Jenkinson, H. F.** 1994. Cell surface protein receptors in oral streptococci. FEMS Microbiol. Lett. **121:**133–140.
16. **Kallipolitis, B. H., and H. Ingmer.** 2001. *Listeria monocytogenes* response regulators important for stress tolerance and pathogenesis. FEMS Microbiol. Lett. **204:**111–115.
17. **Keyes, P.** 1958. Dental caries in the molars of rats: a method for diagnosing and scoring several types of lesions simultaneously. J. Dent. Res. **37:**1088–1099.
18. **Kleerebezem, M., L. E. Quadri, O. P. Kulpers, and W. M. de Vos.** 1997. Quorum sensing by peptide pheromones and two-component signal transduction systems in Gram-positive bacteria. Mol. Microbiol. **24:**895–904.
19. **Kolenbrander, P. E., and J. London.** 1993. Adhere today, here tomorrow: oral bacterial adherence. J. Bacteriol. **175:**3247–3252.
20. **Konig, J., A. Bock, A. L. Perraud, T. M. Fuchs, D. Beier, and R. Gross.** 2002. Regulatory factors of *Bordetella pertussis* affecting virulence gene expression. J. Mol. Microbiol. Biotechnol. **4:**197–203.
21. **Kuramitsu, H. K.** 1993. Virulence factors of mutans streptococci: role of molecular genetics. Crit. Rev. Oral Biol. Med. **4:**159–176.
22. **Lee, S. F., A. Progulske-Fox, G. W. Erdos, D. A. Piacentini, G. W. Ayakawa, P. J. Crowley, and A. S. Bleiweis.** 1989. Construction and characterization of isogenic mutants of *Streptococcus mutans* deficient in major surface protein antigen P1 (I/II). Infect. Immun. **57:**3306–3313.
23. **Levin, J. C., and M. R. Wessels.** 1998. Identification of *csrR*/*csrS*, a genetic locus that regulates hyaluronic acid capsule synthesis in group A *Streptococcus*. Mol. Microbiol. **30:**209–219.
24. **Li, Y.-H., P. C. Y. Lau, J. H. Lee, R. P. Ellen, and D. G. Cvitkovitch.** 2001. Natural genetic transformation of *Streptococcus mutans* growing in biofilms. J. Bacteriol. **183:**897–908.
25. **Li, Y.-H., P. C. Y. Lau, N. Tang, G. Svensäter, R. P. Ellen, and D. Cvitkovitch.** 2002. Novel two-component regulatory system involved in biofilm formation and acid resistance in *Streptococcus mutans*. J. Bacteriol. **184:**6333–6342.
26. **Loesche, W. J.** 1986. Role of *Streptococcus mutans* in human dental decay. Microbiol. Rev. **50:**353–380.
27. **Loo, C. Y., D. A. Corliss, and N. Ganeshkumar.** 2000. *Streptococcus gordonii* biofilm formation: identification of genes that code for biofilm phenotypes. J. Bacteriol. **182:**1374–1382.
28. **Marmur, J.** 1961. A procedure for the isolation of deoxyribonucleic acid from microorganisms. J. Mol. Biol. **3:**208–218.
29. **Michalek, S. M., J. R. McGhee, and J. M. Navia.** 1975. Virulence of *Streptococcus mutans*: a sensitive method for evaluating cariogenicity in young gnotobiotic rats. Infect. Immun. **12:**69–75.
30. **Munro, C., S. M. Michalek, and F. L. Macrina.** 1991. Cariogenicity of *Streptococcus mutans* V403 glucosyltransferase and fructosyltransferase mutants constructed by allelic exchange. Infect. Immun. **59:**2316–2323.

31. **Murchison, H., S. Larrimore, and R. Curtiss III.** 1981. Isolation and characterization of *Streptococcus mutans* mutants defective in adherence and aggregation. Infect. Immun. **34:**1044–1055.
32. **Novak, J., L. Novak, G. R. Shah, W. A. Woodruff, and P. W. Caufield.** 1997. Transposon mutagenesis: cloning of chromosomal DNA from the site of Tn*916* insertion using polymerase chain reaction. Biotechnol. Tech. **11:**51–54.
33. **Nyad, B., and M. Kilian.** 1990. Comparison of the initial streptococcal microflora on dental enamel in caries-active and in caries-inactive individuals. Caries Res. **24:**267–272.
34. **O'Connell-Motherway, M., D. van Sinderen, F. Morel-Deville, G. F. Fitzgerald, S. D. Ehrlich, and P. Morel.** 2000. Six putative two-component regulatory systems isolated from *Lactococcus lactis* subsp. cremoris MG1363. Microbiology **146:**935–947.
35. **Ooshima, T., M. Matsumura, T. Hoshino, S. Kawabata, S. Sobue, and T. Fujiwara.** 2001. Contributions of three glucosyltransferases to sucrose-dependent adherence of *Streptococcus mutans*. J. Dent. Res. **80:**1672–1677.
36. **Perez-Casal, J., M. G. Caperon, and J. R. Scott.** 1991. Mry, a *trans*-acting positive regulator of the M protein gene of *Streptococcus pyogenes* with similarity to the receptor proteins of two-component regulatory systems. J. Bacteriol. **173:**2617–2624.
37. **Sambrook, J., E. F. Fritsch, and T. Maniatis.** 1989. Molecular cloning: a laboratory manual, 2nd ed. Cold Spring Harbor Laboratory Press, Cold Spring Harbor, N.Y.
38. **Sato, Y., Y. Yamamoto, and H. Kizaki.** 1997. Cloning and sequence analysis of the *gbpC* gene encoding a novel glucan-binding protein of *Streptococcus mutans*. Infect. Immun. **65:**668–675.
39. **Sato, Y., Y. Yamamoto, and H. Kizaki.** 2000. Construction of region-specific partial duplication mutants (merodiploid mutants) to identify the regulatory gene for the glucan-binding protein C gene *in vivo* in *Streptococcus mutans*. FEMS Microbiol. Lett. **186:**187–191.
40. **Senghas, E., J. M. Jones, M. Yamamoto, C. Gawron-Burke, and D. B. Clewell.** 1988. Genetic organization of the bacterial conjugative transposon Tn*916*. J. Bacteriol. **170:**245–249.
41. **Southern, E. M.** 1975. Detection of specific sequences among DNA fragments separated by gel electrophoresis. J. Mol. Biol. **98:**503–517.
42. **Spatafora, G., M. Moore, S. Landgren, E. Stonehouse, and S. Michalek.** 2001. Expression of *Streptococcus mutans fimA* is iron-responsive and regulated by a DtxR homologue. Microbiology **147:**1599–1610.
43. **Spatafora-Harris, G., S. M. Michalek, and R. Curtiss III.** 1992. Cloning of a locus involved in *Streptococcus mutans* intracellular polysaccharide accumulation and virulence testing of an intracellular polysaccharide-deficient mutant. Infect. Immun. **60:**3175–3185.
43a. **U.S. Department of Health and Human Services.** 2000. Oral health in America: a report of the Surgeon General. U.S. Department of Health and Human Services, Washington, D.C.
44. **Verhamme, D. T., J. C. Arents, P. W. Postma, W. Crielaard, and K. J. Hellingwerf.** 2002. Investigation of *in vivo* cross-talk between key two-component systems of *Escherichia coli*. Microbiology **148:**69–78.
45. **Vickerman, M. M., M. C. Sulavik, P. E. Minick, and D. B. Clewell.** 1996. Changes in the carboxyl-terminal repeat region affect extracellular activity and glucan products of *Streptococcus gordonii* glucosyltransferase. Infect. Immun. **64:**5117–5128.
46. **Vickerman, M. M., and D. B. Clewell.** 1997. Deletions in the carboxyl-terminal region of *Streptococcus gordonii* glucosyltransferase affect cell-associated enzyme activity and sucrose-associated accumulation of growing cells. Appl. Environ. Microbiol. **63:**1667–1673.
47. **Yamashita, Y., W. H. Bowen, R. A. Burne, and H. K. Kuramitsu.** 1993. Role of the *Streptococcus mutans gtf* genes in caries induction in the specific-pathogen-free rat model. Infect. Immun. **61:**3811–3817.
48. **Yoshida, A., and H. K. Kuramitsu.** 2002. Multiple *Streptococcus mutans* genes are involved in biofilm formation. Appl. Environ. Microbiol. **68:**6283–6291.
49. **Zahrt, T. C., and V. Deretic.** 2001. *Mycobacterium tuberculosis* signal transduction system required for persistent infections. Proc. Natl. Acad. Sci. USA **98:**12706–12711.

Editor: A. D. O'Brien